Indoor Propagation Measurements with a Reconfigurable Intelligent Surface at 3.5 GHz

Nielsen, Jesper Ødum; Franek, Ondrej; Ying, Zhinong

Published in:
Proceedings of the 18th European Conference on Antennas and Propagation (EuCAP 2024)

Publication date:
2024

Document Version
Accepted author manuscript, peer reviewed version

Indoor Propagation Measurements with a Reconfigurable Intelligent Surface at 3.5 GHz

Jesper Ødum Nielsen*, Ondrej Franek*‡, Ying Zhinong*

*APMS, Dept. of Electronic Systems, Technical Faculty of IT and Design, Aalborg University, Denmark.
Email: {jni, of, zy}@es.aau.dk

‡Department of Radio Electronics, Brno University of Technology, Brno, Czechia

***Abstract*—This paper describes an investigation of the practical impact of a reconfigurable intelligent surface on indoor radio propagation. The evaluation is based on measurements of the instantaneous channel impulse response (CIR) between a static transmitter (Tx) and moving receiver (Rx) antennas in non-line of sight (NLOS), where the reconfigurable intelligent surface (RIS) was placed to potentially improve the channel. Different configurations of the RIS were employed and a mean power gain of up to 22 dB was found when introducing the RIS, but the gain was highly dependent on the distance between the Tx antenna and the RIS as well as the polarization, where gains of only about 1 dB was found for a 5 m distance. Also the correct focus point of the RIS was found to be important for close distances. In addition, statistics of the instantaneous power level were investigated.**

***Index Terms*—reconfigurable intelligent surface, indoor radio propagation, adaptive arrays, beamforming**

I. Introduction

In recent years the concept of RISs has been the attention of much research [1]. Instead of seeing the physical propagation environment as something given that must be taken into account when designing and operating communications systems, the idea is to introduce elements that change the properties of the propagation in desirable ways. A RIS consists of a large number of elements, each of which can receive an incoming field an re-radiate with a configurable phase change. This allows to control where in the physical environment the phases of the contributions align, and thus focusing and creating low/high power regions at desired points is possible.

One vision is to employ RISs to help providing network coverage in difficult to reach areas as an alternative to deploy more base stations in, *e.g.*, beyond 5G networks. A RIS can potentially be relatively large and passive (in the sense of not having amplifiers), implemented at low cost compared to a base station and provide energy savings. The RIS could optionally be dynamic and controlled according to needs. The application of RIS technology in practice is still at an early stage where prototypes are evaluated, *e.g.* in [2]. The current work investigates the gains achievable with a specific RIS in some practical indoor setups where the RIS may act as a reflector to improve signal strength. Measurements of the CIR are performed for moving antennas and the instantaneous channel amplitude is evaluated both in terms of mean power and distribution for various RIS settings.

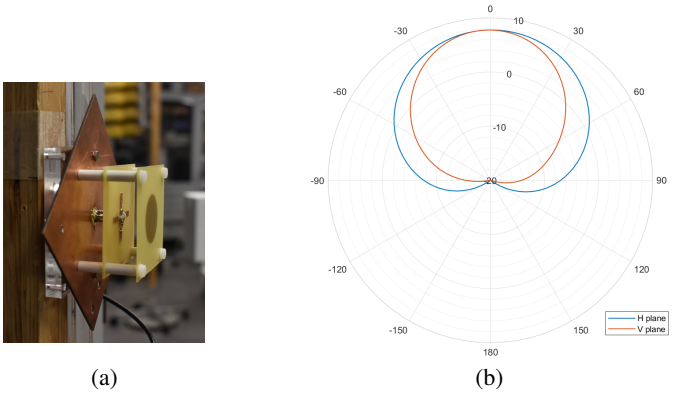

(a) (b)

Fig. 1. (a) The dual-polarized patch antenna and (b) the gain patterns.

II. Measurements

All measurements were carried out using the wide-band correlation channel sounding system system described in [3], configured to operate in a 100 MHz band centered at 3.5 GHz and sounding a 2×4 (Tx $\times$ Rx) branch multiple-input multiple-output (MIMO) channel. The two Tx channels Tx1 and Tx2 are sounded simultaneously and connected to the vertical and horizontal ports, respectively, of a dual-polarized antenna, see Fig. 1. The 4 Rx antennas were connected to a single frontend of the sounder via fast switch. Below a set of CIR measurements for all 2×4 branch combinations is denoted a channel *snapshot*, which was completed in 320 μs.

The four Rx printed circuit board (PCB) antennas are identical with dipole-like characteristics and mounted to be vertically polarized and with a radiation pattern which is approximately omni-directional in azimuth.

The RIS used was the model I24-S35 from Beijing Actenna Technology Co, Ltd. which is specified to operate in the 3.4–3.6 GHz band with a 1–3 dB insertion loss. Its elements are arranged in a 10×10 planar grid and the phase of individual elements can be set in steps of 90° with an accuracy of $\pm 15°$, *i.e.*, 2-bit control. It supports dual-linear polarization, with the same phase shift applied to both polarizations. It is noted that the polarizations of the incident and reflected fields are orthogonal. The unit size is $430 \times 430 \times 46\,\text{mm}^3$ and was

Presented at the *18th European Conference on Antennas and Propagation (EuCAP 2024).*

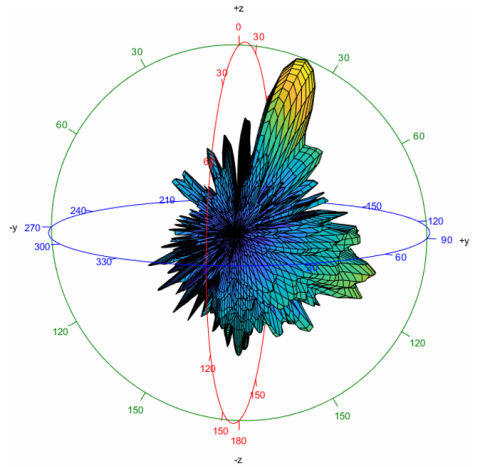

Fig. 2. Power gain pattern of the RIS antenna, configured for AoD $\theta = 20°$, $\phi = 90°$ and AoA $\theta = 40°$, $\phi = -90°$.

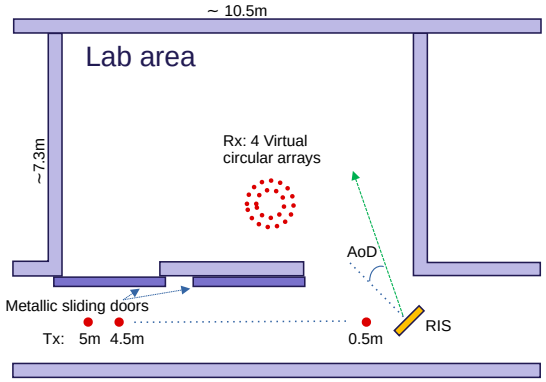

Fig. 3. Sketch of the laboratory area where the measurements took place (not to scale).

controlled from a computer via a serial link. An example of a beam pattern is given in Fig. 2.

All measurements took place in the laboratory area of Antennas, Propagation and Millimetre-Wave Systems (APMS) section at Aalborg University, as sketched in Fig. 3. The Tx was located in a corridor to which the lab area is connected through openings, one of which is closed by a sliding door. The RIS was placed just outside the other opening, so that it could potentially scatter signal from the corridor into the lab area where the Rx antennas were. The lab is furnished with tables, shelves and closets filled with equipment and miscellaneous other items, see Fig. 4.

A measurement consists of a series of 349 snapshots acquired while the Rx antennas were moved in concentric circles by a pedestal rotating a block of expanded polystyrene foam (EPS) on which the antennas were mounted, see Fig. 4. In this way, each Rx antenna formed a virtual circular array (VCA) with radius of 10 cm, 18 cm, 26 cm, 37.5 cm, respectively, corresponding to about 1.1–4.4 wavelengths. The angle increment between snapshots was constant, *i.e.*, about 1° and the time used for a measurement was about 39 s. Note that the measurements without the RIS was, for practical reasons,

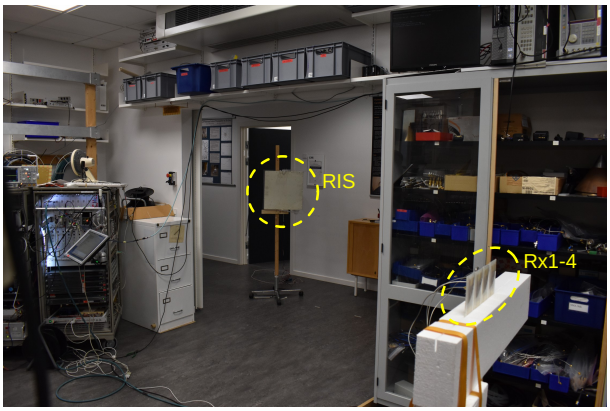

Fig. 4. The laboratory area where the measurements took place.

done with an angle increment of 3° in an otherwise essentially identical setup. In this setup the measurement time was about 232 s since more (6360) snapshots were obtained.

The Tx antenna, the Rx antennas and the RIS center were all mounted at a height of 1.25 m from the floor. Further, the RIS was mounted so that its normal was at an angle of 40° from the center line of the corridor, which made the normal point at the center of the VCAs.

Although the RIS can be used to form beams in a two-dimensional angle space, this work only uses main directions located in the horizontal plane at a height of 1.25 m, with the direction defined by the angle from the RIS normal, as shown in Fig. 3. In all the measurements, the RIS angle of arrival (AoA) is $-40°$, which is the direction of the Tx antenna.

In the following d denotes the distance in meter between the RIS and the Tx, and d_f denotes the focal distance, *i.e.*, the distance used when computing the phase values for the RIS configuration regarding the AoA. The similar focal distance used towards the Rx to control the angle of departure (AoD), was always set to 5 m. Two series of measurements were carried out, as described below.

Angle:
: For fixed $d = d_f = 0.5$, measurements were made for the AoDs $-15°, -10°, 0°, 20°, 40°$.

Dist:
: The AoD was set to 0°. Measurements were made for $d \in \{0.5, 1.0, \ldots, 5.0\}$ with both $d_f = d$ and $d_f = 5$. In addition, for each distance a measurement was done without the RIS. Further, for distances $d = 1.5$ and $d = 5.0$, the RIS was also configured with all elements set to zero phase, random values, and the RIS powered off (but present).

III. Data Analysis

For each combination of Tx branch and Rx branch, the measured CIR can be represented as $h'(s,n) = h(s,n) + w(s,n)$, where s and n denote the discrete snapshot and delay index, respectively, and where $h(s,n)$ is the CIR sample and $w(s,n)$ is the noise component. The delay samples are given by $\tau(n) = n\Delta_\tau$ with $n \in \{0, 1, \ldots, N-1\}$, $\Delta_\tau = 2.5$ ns and

$N = 960$. The snapshot index $s \in \{0, 1, \ldots, S-1\}$ corresponds to the VCA element number with $S = 349$ or $S = 6360$ for the measurements with or without the RIS, respectively. Note that Tx and Rx branch indices are omitted in the following description for brevity, since the processing was done on all combinations independently.

When processing the data it is essential to consider the noise that inevitably will be present in the measured CIR data. The rest of this section is adapted from [4] where a similar processing is described (for other measurements), with the purpose of ensuring the quality of the processed data.

Despite the use of automatic gain control (AGC) in the measurement system, a high signal to noise ratio (SNR) cannot be guaranteed in all the measurements, due to the highly dynamic channel. In this work the approach is to estimate the SNR for each CIR snapshot and only include snapshots that have an SNR above a threshold of 15 dB. Although very few snapshots in the current measurement campaign have too low SNR, the following procedure is followed to control the quality.

The instantaneous SNR for snapshot s is estimated by

$$\eta(s) = 10 \log_{10} \left[\frac{P_h(s)}{P_w(s)} \right] \tag{1}$$

where the signal and noise power are estimated, respectively, as

$$\begin{aligned} P_h(s) &= \sum_{n=0}^{M-1} |h(s,n)|^2 - M\tilde{\sigma}_w^2(s) \\ P_w(s) &= M\tilde{\sigma}_w^2(s) \end{aligned} \tag{2}$$

where the signal is assumed to be contained in the first $M = 135$ samples of the CIR, corresponding to 338 ns. This was verified by visual inspection of the data. The estimated instantaneous noise density is

$$\tilde{\sigma}_w^2(s) = \frac{1}{K} \sum_{n=0}^{K-1} |h(s, N-n)|^2 \tag{3}$$

i.e., it is estimated from the last $K = 460$ samples of each CIR. Visual inspection reveals that in this part of the CIR the squared magnitude of the samples may be modeled by fluctuations around a mean value, consistent with the assumption that, due to path loss, any signal components in this delay range are much lower than the system noise.

The SNR estimation described above is done for all combinations of Tx branch index, Rx branch index and snapshot. The subsequent processing only considers data with an SNR above the threshold of 15 dB.

Narrowband channels are considered in this work, and hence a discrete Fourier transform (DFT) is applied to the measured CIRs. The sub-channels are all normalized individually over the snapshots, as

$$H_n(c,t,r,s) = H'(c,t,r,s) / H_{\text{sys}}(c) \tag{4}$$

in which $H'(c,t,r,s)$ is the channel transfer function before normalization, where c, t, r is, respectively, the sub-channel, transmitter, and receiver index. $H_{\text{sys}}(c)$ denotes the known system transfer function. Only a subset of the sub-channels are included in the analysis, chosen to be within a 3 dB bandwidth of 70 MHz, corresponding to $C = 168$ sub-channels. The subsequent analysis is based on vectors of the channel coefficients obtained by concatenating the coefficients for all combinations of sub-channels, $R = 4$ Rx-indices, and snapshots. For a single measurement this leads to a maximum of $C \cdot R \cdot S = 168 \cdot 4 \cdot 349 = 234{,}528$ samples, when all the corresponding SNRs are above the threshold.

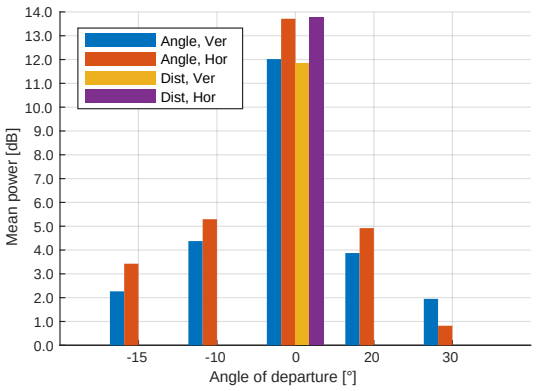

Fig. 5. Mean normalized power versus the AoD, where the LOS is 0°.

The vector of complex coefficients is used to compute an empirical cumulative distribution function (CDF) of the power gain, where the coefficients are normalized to the mean value for each measurement. To ease comparisons, both the mean value and the 1st percentile is used, *i.e.*, the level, in dB, below which 1% of the power gain samples are observed. In the following 'power' is used as a shorthand for channel power gain.

It is noted that the sub-channels for a measurement may be correlated, depending on the channel properties, and hence the coefficients are not necessarily of the same value in the analysis. Note also, that the lowest power levels in the CDF are not limited by the applied SNR threshold, since the power in the sub-channels are subject to fading and the SNR is determined by the total power in the wideband channel.

IV. Results and Discussion

A. Mean Gain

Fig. 5 displays the mean power versus the AoD from the RIS. In all cases the gains are normalized to the mean gain value achieved for vertical Tx polarization at 1.5 m for the scenario without the RIS. Most of the measurements shown are from the Angle series of measurements, but for 0° AoD a measurement is also available from the Dist series, since the two series both include the distance 0.5 m. The results obtained are almost identical (within 0.2 dB) with a gain of approximately 12 dB and 13.7 dB achieved for vertical and horizontal polarization, respectively. For each angle the gain is 0.9-1.7 dB higher for horizontal than for vertical polarization,

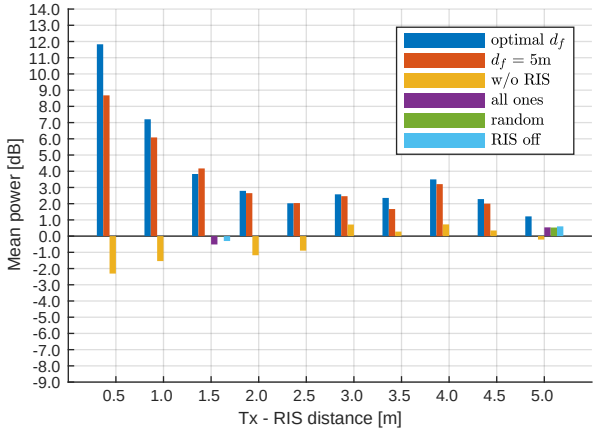

(a) Vertical Tx polarization

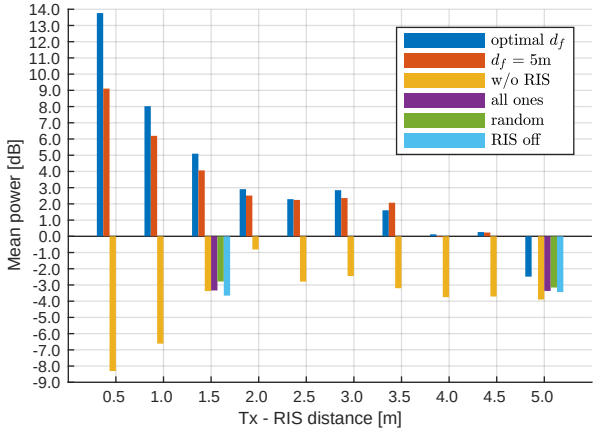

(b) Horizontal Tx polarization

Fig. 6. The normalized measured mean power versus distance between the Tx antenna and RIS for (a) vertical and (b) horizontal Tx polarization. The different bar/colors are for the different configurations of the RIS.

except at 30° where the vertical polarization is about 1.1 dB higher.

The gain is strongly dependent on the AoD, with a decrease of 7.6–8.4 dB at −10° compared to the gain at 0° and even more at larger angles. Since an AoD of 0° is in the direction of the VCA, this is the expected impact of the RIS.

The mean power versus distance is shown in Fig. 6, obtained from processing the measurements in the Dist series. Again all power values are normalized to the mean value for the case without the RIS, at 1.5 m for vertical polarization. The different colors represent the configurations of the RIS.

The power without the RIS is noticed to be varying some 3.0 dB (7.5 dB) along the corridor for the vertical (horizontal) Tx polarization. The relatively low variation with distance may be due to the setup, where the corridor may guide the signal before entering the lab area.

Without the RIS, the power for the horizontal Tx polarization is low, in the range about −8.3 to −0.8 dB, since the gain of the Rx antenna is included and the Rx antenna is mainly vertically polarized. Thus, in this case the Rx power is likely due to the cross-polarization coupling in the channel in addition to minor cross-polarization parts from the antennas.

The power achieved with the RIS is generally largest for close distances. This is expected since at short distances the RIS will reflect a large part of the power emitted by the Tx antenna, but at larger distances more of the power is reaching parts of the environment outside the RIS where it has no impact.

Defining the gain as the difference between the power achieved with and without the RIS for each distance, the gain is seen to depend highly on the distance. For 0.5-1.5 m the gain is 3.8–14.1 dB for the configuration with optimum focal distance, while the gain is 1.4–4.0 dB for 2–5 m distance, both for the vertical polarization. For horizontal polarization, the gain is about 8.5–22.1 dB for 0.5-1.5 m distance and 1.4–5.3 dB for 2–5 m, again for optimum focal distance. The generally higher gain for horizontal versus vertical Tx polarization is due to the Rx antenna being mainly vertically polarized and the wave reflected by the RIS is orthogonal to the incoming wave. Hence, in this setup the RIS effectively increases the cross-coupling in the channel.

The power achieved when assuming a focal distance of 5 m versus using the optimal distance, *i.e.*, the actual distance, shows some differences, where the optimum focal distance gives −0.3 dB to 3.1 dB (1.0 dB to 4.7 dB) higher gain at 0.5–1.5 m, but only 0–0.7 dB (−0.5 dB to 0.5 dB) at longer distances for vertical (horizontal) polarization. The RIS element phase configuration is a function of the path length from the Tx to each element, but for sufficiently large Tx-RIS distance, the phase variation with distance is too small to cause practical differences, since the RIS can only be configured in 90° steps.

For the 1.5 m and 5 m distances measurements were also made with non-beamforming configurations of the RIS; viz. ‘random’, ‘all-ones’, and ‘RIS off’. For these cases the results are similar to those obtained without the RIS, within about 0.8 dB.

B. 1st Power Percentile

Fig. 7 shows the 1st percentile of the channel power gain versus the AoD for both polarizations obtained from the Angle measurement series. For comparison, the measurements from the Dist measurement series are shown for the 0° AoD. It is noticed that the results for the two series match within about 0.3 dB.

For 0° AoD in the horizontal polarization the percentile is about −14 dB compared to values mostly below −19 dB for other AoDs. This is consistent with the RIS creating a dominant direction in the horizontal polarization when the AoD is towards the VCA, whereas other AoDs make scattering from other directions more important.

Fig. 8 displays how the 1st percentile depends on the distance for both Tx polarizations. For all distances and RIS configuration the percentiles for vertical polarization are relatively low in the range −21.5 dB to −19 dB with most values below −20 dB. Thus, the channels have statistics comparable to the −20 dB 1st percentile of a Rayleigh channel. Further, the variation due to the RIS configuration is within about 1.7 dB

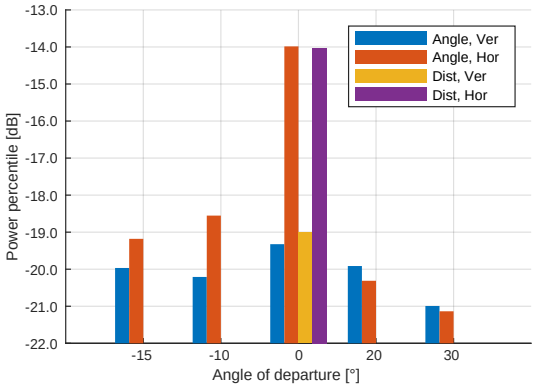

Fig. 7. 1st percentile of the measured instantaneous NB channel power gain versus the AoD, where the LOS direction between the RIS and the Rx is at 0°.

when the case of no RIS is included. It is noticed that even for $d < 2$ m where the mean power is higher than at longer distances (see Fig. 6(a)), the percentiles are -19 dB or below, indicating that the higher mean power is due to an increased power of more than just a few dominant paths.

The picture is different in case of horizontal Tx polarization. For $d \leq 2$ the percentiles are in the range -14 to -18.5 dB indicating that a dominating path exists from the RIS where the outgoing polarization matches that of the vertically polarized Rx antennas. For $d > 2$ the percentiles obtained with the RIS are in the range -21.0 to -19.0 dB and within about 2 dB of the similar measurements without the RIS. Thus, although the mean power increases due to the RIS also for these distances, this is not only due to a increase power in a few paths.

V. Conclusions

The gain of using the RIS is defined here as the difference in dB between the measured channel power gain with and without the RIS present. The observed gains were strongly dependent on the distance between the Tx antenna and the RIS. For distances 0.5–1.5m the gains were 3.8–14.1 dB for vertical polarization of the Tx, while only 1.4–5.3 dB for 2–5 m distances. This observation can be attributed to the relatively small RIS surface area, compared to the total area illuminated by the antenna. For horizontal polarization Tx the gains were generally higher, in the range 8.5–22.1 dB for 0.5–1.5m distances and 1.4–5.3 dB for 2–5 m distances. This is likely due to the incident and reflected fields being orthogonal for the RIS employed in the measurements.

The impact of using the optimum focal distance for the RIS configuration was also studied, and up to 4.7 dB higher gains for 0.5–1.5 m physical distances were found compared to using a fixed 5 m focal distance. However, at longer distances the differences were small.

Also statistics of the instantaneous gains where studied in terms of the 1st percentile. For vertical polarization the percentiles were about -21.5 dB to -19 dB. This indicates that the higher mean power for distances below 2 m is due to an increased power of more than just a few dominant paths. For horizontal polarization, the percentile was -14 dB to -18.5 dB, consistent with the RIS creating dominant paths.

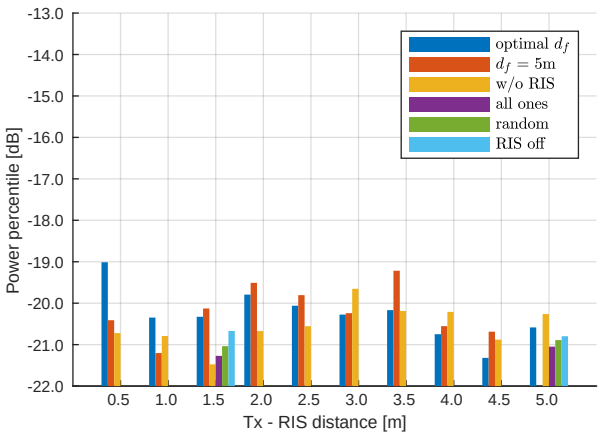

(a) Vertical Tx polarization

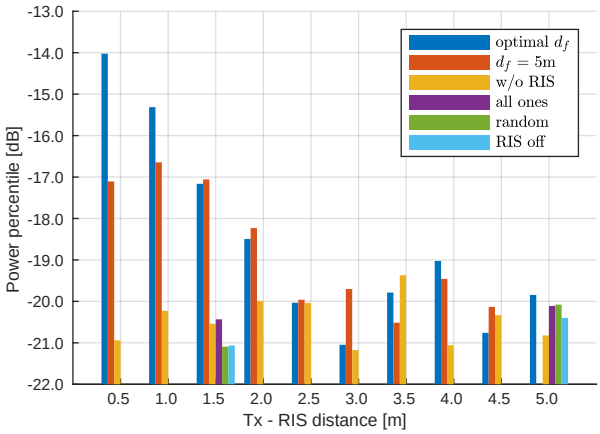

(b) Horizontal Tx polarization

Fig. 8. 1st percentile of the measured instantaneous NB channel power gain versus distance d between the Tx antenna and RIS for (a) vertical and (b) horizontal Tx polarization. The different bar/colors are for the different configurations of the RIS.

Acknowledgment

This work was supported by the EU H2020 Reconfigurable Intelligent Sustainable Environments for 6G Wireless Networks (RISE-6G) project number 101017011.

References

[1] E. Björnson, O. Özdogan, and E. G. Larsson, "Reconfigurable intelligent surfaces: Three myths and two critical questions," *IEEE Communications Magazine*, vol. 58, no. 12, pp. 90–96, 2020.

[2] X. Pei, H. Yin, L. Tan, L. Cao, Z. Li, K. Wang, K. Zhang, and E. Björnson, "RIS-aided wireless communications: Prototyping, adaptive beamforming, and indoor/outdoor field trials," *IEEE Transactions on Communications*, vol. 69, no. 12, pp. 8627–8640, 2021.

[3] J. Ø. Nielsen, W. Fan, P. C. F. Eggers, and G. F. Pedersen, "A channel sounder for massive MIMO and MmWave channels," *IEEE Commun. Mag.*, vol. 56, no. 12, pp. 67–73, December 2018.

[4] J. Ødum Nielsen and G. Frølund Pedersen, "Amplitude distributions of measured 21.5 GHz indoor channels for a handheld array," in *2021 15th European Conf. Antennas and Propagation (EuCAP)*, 2021, pp. 1–5.